

## Research Article

## Optimization of process parameters during Friction Stir Welding of Aluminium 5083 & 6082 Alloys

Yeswanth Kumar Y<sup>Å</sup>, Aditya Kumar<sup>Å</sup> and Rajyalakshmi<sup>Å</sup><sup>Å</sup>Mechanical Engineering Department, VIT University, Vellore, Tamil Nadu, India

Accepted 17 Dec 2014, Available online 20 Dec 2014, Vol.4, No.6 (Dec 2014)

### Abstract

The paper deals with the optimization of welding parameters of friction stir welding of different Aluminium alloy groups. For this purpose 5 series Aluminium alloy Al 5083 and 6 series Aluminium alloy Al 6062 were taken. Tensile Strength test and micro structure analysis under various rotating speeds and tool profiles is conducted. It is observed that the increase in tool rotation speed and the tool axial force result in increase of ultimate tensile strength (UTS) up to a maximum value. In-significant effects of the tool profile at low welding speeds are noticed. At higher speeds square tool profile achieves higher strength than that of circular tool profile.

**Keywords:** Friction stir welding, Aluminium Alloys, Process parameters, microstructure, mechanical properties.

### 1. Introduction

Friction stir welding, a solid state joining technique invented in 1991 by The Welding Institute (TWI), is extensively used in the joining of Al, Mg, Cu, Ti and their alloys. This technique has been extended to dissimilar welding of the above-mentioned alloys and also to the welding of steels. A relatively new joining process, friction-stir welding uses no filler materials and can join alloys of aluminium, copper, magnesium, zinc, steels and titanium. It sometimes produces a weld that is stronger than base material. Melting does not occur and joining takes place below the melting temperature of the base material, a high-quality weld is created. This characteristic feature of this welding process greatly reduces the ill effects of high heat input, including distortion and eliminates solidification effects. It also produces no fumes and highly efficient which makes this process environmental friendly.

The process of FSW has been widely used in the aerospace, shipbuilding, automobile industries and in many application of commercial importance. This is because of many of its advantages over the conventional welding techniques some of which include very low distortion, no fumes, porosity or spatter, no consumables (no filler wire), no special surface treatment and no shielding gas requirement. FSW joints have improved mechanical properties and are free from porosity or blow holes compared to conventional welded materials. At the end of the welding process an exit hole is left behind when the tool is withdrawn which is undesired in most of the applications. This has been overcome by providing an offset in the path for continuous trajectory, or by

continuing into a dummy plate for non-continuous paths, or simply by machining off the undesired part with the hole. Large down forces and rigid clamping of the plates to be welded are a necessity for this process, which causes limitation in the applicability of the process to weld jobs with certain geometries.

Friction stir welding (FSW) is a solid-state, hot-shear joining process in which a rotating tool with a shoulder and terminating in a threaded pin, moves along the butting surfaces of two rigidly clamped plates placed on a backing plate. The shoulder makes firm contact with the top surface of the work-piece. Heat is generated between the tool and the material which leads to a very soft region near the FSW tool. Severe plastic deformation and flow of this plasticized metal occurs as the tool is translated along the welding direction. Material is transported from the front of the tool to the trailing edge where it is forged into a joint.

It was experimentally proven at The Welding Institute, UK. FSW has evolved as a technique of choice in the routine joining of aluminium components. Its applications for joining difficult metals and metals other than aluminium are growing at a slower pace. There have been widespread benefits resulting from the application of FSW in for example, aerospace, shipbuilding, automotive and railway industries. FSW involves complex interactions between varieties of simultaneous thermo-mechanical processes. The interactions affect the heating and cooling rates, plastic deformation and flow, dynamic recrystallization phenomena and the mechanical integrity of the joint. A typical cross-section of the FSW joint consists of a number of zones. The heat-affected zone (HAZ) is similar to that in conventional welds although the maximum peak temperature is significantly less than the solidus temperature and the heat-source is rather diffuse.

\*Corresponding author: Yeswanth Kumar Y

**Table 1:** Chemical composition of Al 5083

Element	Si	Fe	Cu	Mn	Mg	Zn	Ti	Cr	Al
%present	0.4	0.4	0.4	0.4-1.0	4.0-4.9	0.3	0.2	0.05-0.25	Balance

**Table 2:** Chemical composition of Al 6082

Element	Si	Fe	Cu	Mn	Mg	Zn	Ti	Cr	Al
% present	0.7-1.3	1	0	0.40-1.00	0.60-1.20	0	0	0.3	Balance

**Table 3:** Welding parameters of circular cutting tool profile

S.No	Metals		Rotating speed(rpm)	Feed (mm/min)	Tool Profile
1	AL 5083	AL 6082	710	20	Circular
2	AL 5083	AL 6082	1000	20	Circular
3	AL 5083	AL 6082	1400	20	Circular

**Table 4:** Welding parameters of Square pin tool profile.

S.No	Metals		Rotating speed(rpm)	Feed (mm/min)	Tool Profile
1	AL 5083	AL 6082	710	20	Square
2	AL 5083	AL 6082	1000	20	Square
3	AL 5083	AL 6082	1400	20	Square

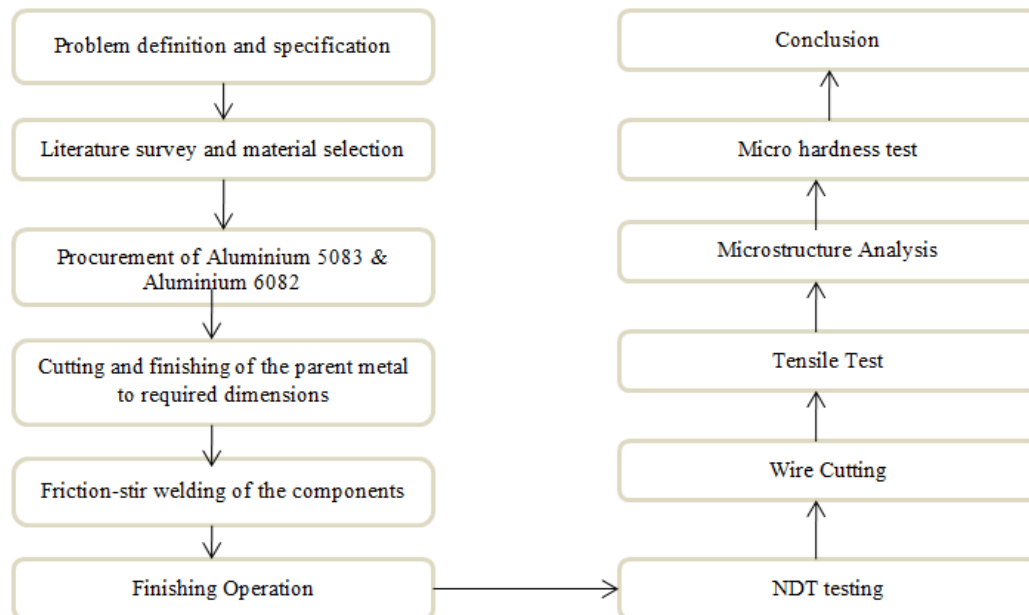


**Fig.1** Flow chart detailing the Process flow

This can lead to somewhat different microstructures when compared with fusion welding processes. The central nugget region containing the “onion ring” appearance is the one which experiences the most severe deformation and is a consequence of the way in which a threaded tool deposits material from the front to the back of the weld. The thermo-mechanically affected zone (TMAZ) lies between the HAZ and nugget; the grains of the original microstructure are retained in this region, but often in a deformed state. A unique feature of the friction stir welding process is that the transport of heat is aided by the

plastic flow of the substrate close to the rotating tool. The heat and mass transfer depend on material properties as well as welding variables including the rotational and welding speeds of the tool and its geometry. In FSW, the joining takes place by extrusion and forging of the metal at high strain rates.

**2. Experimental Procedure**

The procedure involves in a variety of the tests which are necessary to determine the properties, as listed in the Flowchart (fig.1).

Welding of dissimilar aluminium alloys AL 5083 and AL 6082 is carried out using milling machine. Here the feed is given constant for all the process. The varying parameters are tool pin profile and rotating speed of cutting tool. The Chemical composition and parameters are given in the following tables for different welding process.

Finishing process is carried out to remove the continuous chips formed on the metals due to welding and to carry out the tests effectively.

During welding process of a sample with the parameters 1400 rpm and 20 mm/min feed the square pin profile with side of length 3.85 mm is broken. Thus the dimension of square pin profile is modified to side of length 5mm.

2.1 N.D.T (Non Destructive Test)

Non-Destructive test is carried out on all the welded specimens by Liquid Penetrant Testing method and Radiographic testing and the welds were found to be clean without any cracks and surface defects.

2.2 Tensile Test

To determine the tensile strength of the stir zone, tensile test specimens were sectioned in the longitudinal direction along the weld line with an electrical discharge machine (EDM). Surfaces were prepared by standard metallographic techniques and etched with Keller’s reagent. The tensile properties and fracture locations depend mainly on the welding defects and hardness of the joint. When the joints are free from defects, their tensile properties are controlled by hardness and fracture occurred in the heat affected zone (HAZ) on the side that show minimum hardness.

These results show better properties at 20 mm/min and this may be due to the sufficient heat generation to fill the pores in time. Lower welding speed resulted in higher temperature and slower cooling rate in the weld zone, which causes grain growth.

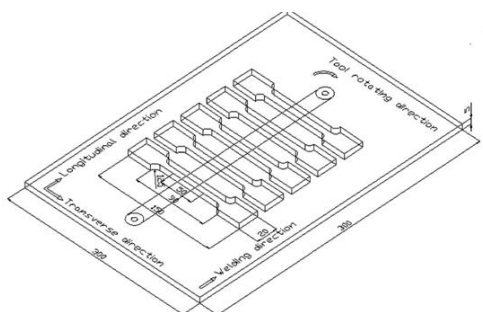


Fig.2 Scheme of extraction of tensile specimen

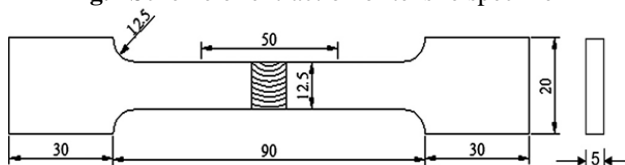


Fig.3 Dimensions (mm) of flat tensile specimen Standards-(ASTM E8M-04)

Friction stir welding (FSW) results in significant microstructural evolution within and around the stirred zone, i.e., nugget zone, Thermo-Mechanical affected zone (TMAZ) and Heat affected zone (HAZ). This leads to substantial change in post weld mechanical properties. During friction stir welding, the temperature rises to about 400-500°C in the nugget zone. This rise causes dissolution and/or overaging of these precipitates in the welds. Since, the heat input during welding increases with increasing tool rotational speed therefore the amount of dissolution of precipitates and degree of overaging also increase proportionally. Also, increasing tool rotations leads to turbulence in the weld joint and can result in insufficient consolidation of the plasticized material and thereby degradation of strength of joints formed with higher tool rotations. Besides, simulation of FSW process has also indicated degradation of joint quality with increasing tool rotational speed due to a serious increase in weld flash. In contrast, heat input decreases with increasing welding speed as the time of interaction between tool and work pieces is reduced and hence, frictional heat generated per unit length of weld is also reduced. Therefore, an increase in strength is observed. Also, welding speed is a more significant factor than rotational speed.

2.3 Microstructure Examination

Microstructures of parent materials and welds were examined by optical microscope. Following friction stir welding, sections were cut from the weld zone to expose the flow pattern geometries. Initially the samples were grinded successively on SiC papers of grit 400 to 1000. After which they were polished on a fine cloth using a 1µm diamond paste to obtain a mirror finish. These sections were polished and etched using a Keller’s reagent (nominally 150 ml water, 3 ml nitric acid, 6 ml hydrochloric acid, and 6 ml hydrofluoric acid).

2.4 Micro Hardness Test

The hardness profiles can assist the interpretation of the weld microstructures and mechanical properties. Micro hardness tests were performed in order to characterize the hardness profile in the vicinity of the weld affected area. The micro hardness tests were performed on a cross section perpendicular to the weld line, at mid thickness across the weld zone and into the parent material.

The Vickers hardness profile of the weld zone was measured on a cross section and perpendicular to the welding direction using a Vickers indenter with a 100gf(gram force) load for 10sec. The hardness profiles are measured along the centreline of the cross section of the welds with various welding speeds. The base metals have a very wide range of hardness, approximately from 75 to 95 HV. The base metals had a hypoeutectic Al/Si microstructure. The Al solid solution, which is softer than the Si solid solution, has a large volume fraction.

3. Results and Discussions

3.1 Tensile Test

The tests results are detailed with the graphs which depict the properties.

**Table 5:** Results of tensile tests of FSW joints at various welding speeds and tools of specimen 1

S.No	Tensile strain at Maximum Load (%)	Load at Break (Standard) (kN)	Tensile stress at Break (Standard) (MPa)	Comment
1	3.16608	0.16	7.41	1400 rpm
2	4.36488	0.19	8.79	1000 rpm
3	1.4778	0.34	18.46	710 rpm
4	1.31079	3.97	131.53	710 rpm
5	3.52269	0.59	20.59	1000 rpm
6	1.59567	0.06	2.13	1400 rpm
Maximum	4.36488	3.97	131.53	
Mean	2.38317	0.78	27.7	
Minimum	1.31079	0.06	2.13	

**Table 6:** Ultimate tensile strength (UTS) and Tensile Strain

	Maximum Load (N)	UTS (GPa)	Modulus (Automatic Young's) (MPa)	Tensile strain at Break (Standard) (%)
1	3616.24956	0.172	32236.71	8.212
2	4568.33839	0.217	37838.172	10.095
3	2360.80885	0.127	27736.425	5.73
4	4060.42337	0.134	28628.576	1.356
5	5074.73946	0.177	30217.429	9.315
6	3813.5767	0.131	28585.659	9.403
Maximum	5074.73946	0.217	37838.172	10.095
Mean	3839.94409	0.153	30091.162	6.861
Minimum	2360.80885	0.127	27736.425	1.356

**Table 7:** Area reduced and the true strain observed at maximum load

	Final Area at Area Reduction (mm <sup>2</sup> )	Initial Area at Area Reduction (mm <sup>2</sup> )	Reduction of Area at Area Reduction (%)	True strain at Maximum Load (mm/mm)
1	15	21.08	28.8425	0.03117
2	15	21.08	28.8425	0.04272
3	15	18.6	19.35484	0.01467
4	15	30.1965	50.32537	0.01302
5	15	28.6677	47.6763	0.03462
6	15	29.16	48.55967	0.01583
Maximum	15	30.1965	50.32537	0.04272
Mean	15	25.56867	39.13237	0.02349
Minimum	15	18.6	19.35484	0.01302

**Table 8:** The percentage Elongation at tensile strength and break

	True stress at Maximum Load (Pa)	% Elongation at Tensile Strength at Non-proportional Elongation (Standard) (%)	% Elongation at Break at Non-proportional Elongation (Standard) (%)
1	176980209	2.85246	8.18454
2	226173656	4.05309	10.06933
3	128800911	0.9958	5.65379
4	136229262	0.75605	0.81345
5	183255257	2.78009	9.23592
6	132867929	1.01582	9.39347
Maximum	226173656	4.05309	10.06933
Mean	156830999	1.88408	6.74868
Minimum	128800911	0.75605	0.81345

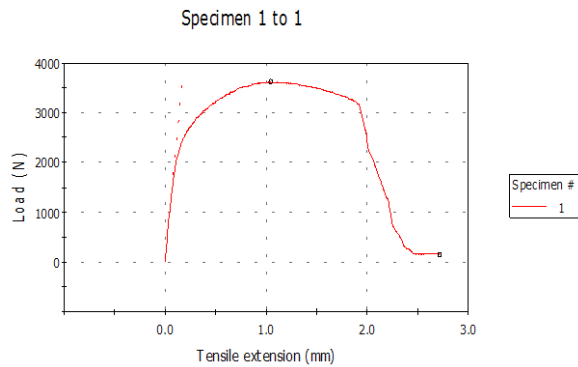


**Fig. 4** Engineering stress-strain diagram of circular pin profile for 1400rpm

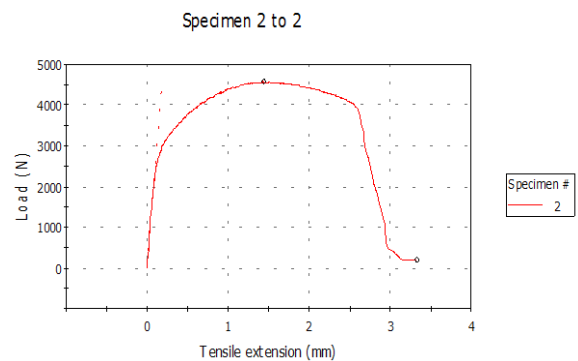


**Fig.5** Engineering stress-strain diagram of circular pin profile for 1000rpm

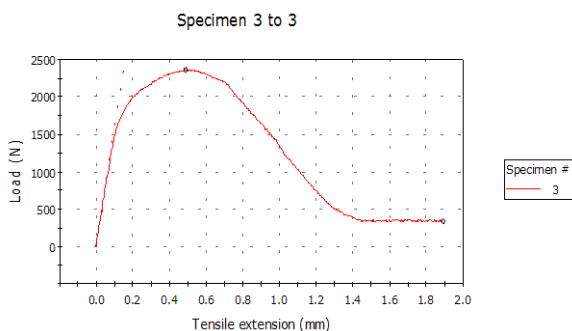


**Fig.6** Engineering stress-strain diagram of circular pin profile for 710rpm

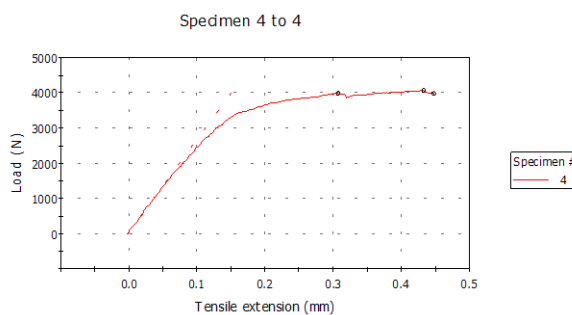


**Fig.7** Engineering stress-strain diagram of square pin profile for 1400rpm

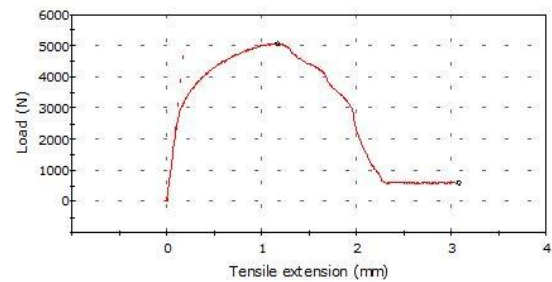


**Fig.7** Engineering stress-strain diagram of square pin profile for 1000rpm

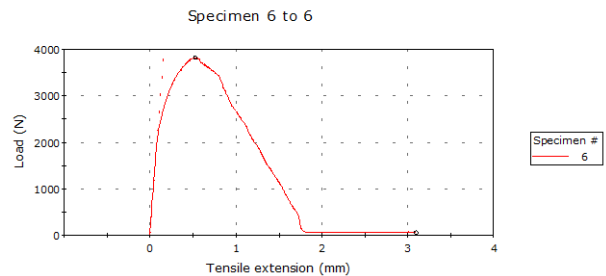


**Fig.8** Engineering stress-strain diagram of square pin profile for 710rpm

We observe the influences of the tool rotation speed on the tensile strength and elongation of the friction stir welded plates. For the friction stir welded plates, a maximum tensile strength of about 217 MPa was obtained at the tool rotation speed of 1000 rpm, which was about 66% of the tensile strength of the base metals. The samples showed very low elongation of 3% or less. The elongation did not significantly change as a function of the tool rotation speed, although a maximum elongation of about 3% was obtained at 1000rpm. The true stress vs true strain curves of the welded materials tested transversely in tension. The curves exhibit a classical elastic-plastic behaviour and the mechanical properties, compared to the parent metals. The joint exhibits very good properties of yielding, ultimate tensile strength and ductility from a global point of view even if the weld has lower 0.2% proof stress and elongations compared to the base metals. In evaluating friction stir welding, critical issues include microstructure control and localized mechanical property variations. The average tensile strength,  $\sigma_b$ , of three as-welded joints was 198 MPa, which was lower than those of the parent metals. It was found that all joints fractured on A5083 side where the hardness was minimal.

We observe that the increase in tool rotational speed, welding speed and tool axial force result in the increase in UTS of the FS welded joints up to a maximum value. The lower rotational speeds, higher welding speeds and lower axial forces (lower heat input condition) produce inadequate heat due to lower friction, which results in poor plastic flow and formation of defects in welded zone(WZ).The defects act as a crack initiation location during tensile test and so, the UTS is lower. The higher rotational speeds, lower welding speeds and higher axial forces (higher heat input condition) produce sufficient heat for metallurgical phenomena such as grain coarsening, solubilisation and coarsening of strengthening precipitates at the WZ, and lowering of dislocation density that

Specimen 5 to 5

decrease the UTS value .We observe that in high heat input condition the number of participates is lower due to dissolution of them, where the size of participates is larger due to growth of them. Larger and fewer participates cause to easier dislocation movement during tensile test in comparison with smaller and more participates and hence, the UTS is lower.

The effect of the tool profile on the tensile strength is examined. Insignificant effect of the tool profile at low welding speed is noticed. At higher welding speed of 20 mm/min, the square profile achieves higher strength compared to the circular one. The achieved higher strength using the square profile at 20 mm/min may be due to the produced higher pulses/s than that produced by the circular one. The higher number of pulsating action produces finer grained microstructure with uniformly distributed precipitates (CuAl<sub>2</sub>) and in turn yields higher strength and hardness. Moreover, the behaviour of the strength at 20 mm/min for the different tool profiles may be attributed to the stirring effect of the welding tool, which becomes weaker. Otherwise, as the square profile achieved best properties, the effect of the rotation speed on the mechanical properties of the FS-joints is carried out, using square profile, at a constant welding speed of 20 mm/min. Figure 8 shows that the strength as well as the elongation percent has slight improvement at 1000 rpm, while the yield strength has neglected changes. The improvement of the mechanical properties at 1000 rpm may be associated with good stirring action along with uniformly distributed precipitates (CuAl<sub>2</sub>).On the other hand, the strength has the lowest value at a high rotation speed of 1400 rpm that can be attributed to the increase of pores in the nugget zone.

From the above, it can be inferred that the tool profile and welding speed are having influence on tensile properties of the FSW joints. The joints fabricated by square tool profile exhibited superior tensile properties with joint efficiency of 61% compared to other joints, irrespective of welding speed. Though the tensile strength and hardness values are lower than the base metal, the joint efficiency is acceptable one when compared to conventional fusion welding process with low joint efficiency not exceeding 50%.

### 3.2 Microstructure

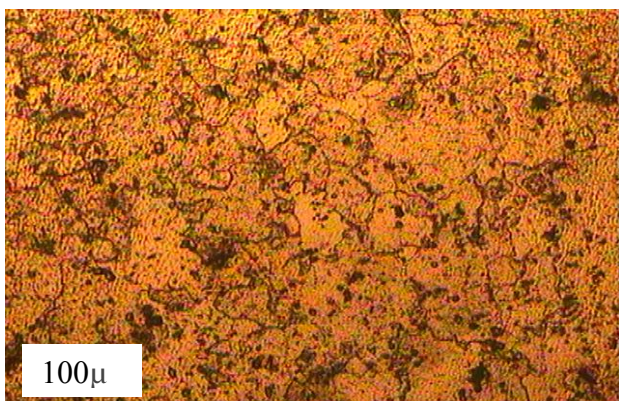


**Fig.9a**Optical microstructures of the stir zone (SZ) with rotating speed 700 rpm (circular profile)

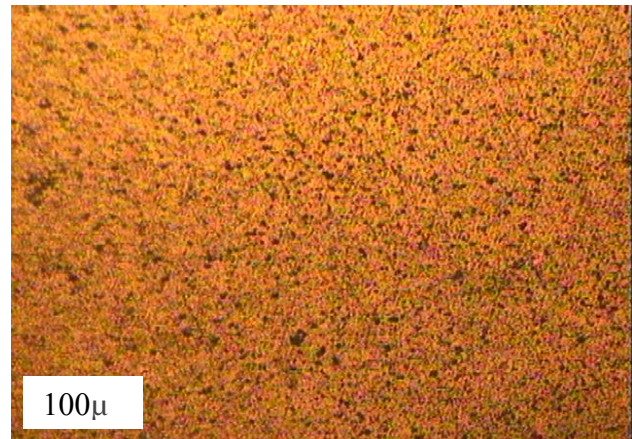


**Fig.9b** Optical microstructures of the stir zone (SZ) with rotating speed 1000 rpm (circular profile)

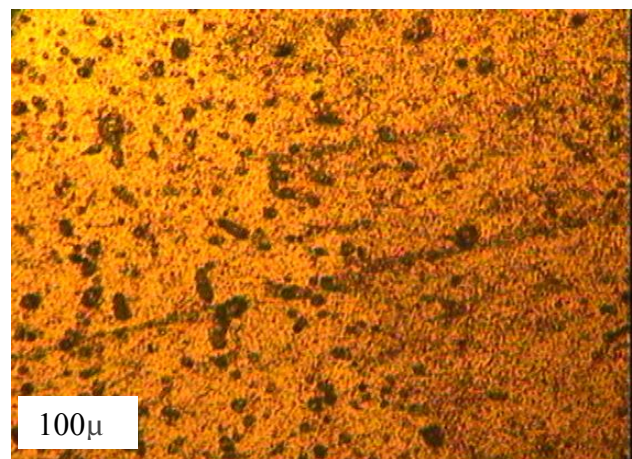


**Fig.9c** Optical microstructures of the stir zone (SZ) with rotating speed 1400 rpm (circular profile).

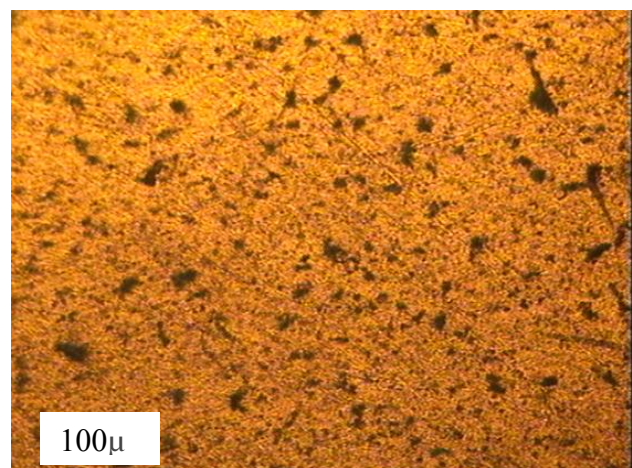


**Fig.9d** Optical microstructures of the stir zone (SZ) with rotating speed 700 rpm (square profile).

In the base metal, the grain size is not uniformed. Namely, non-equiaxed large grains are over 100 μm in size. In contrast, the stir zone is composed of smaller and equiaxed grains. This result suggests that the stir zone is severely plastically deformed by mechanical stirring action of the rotating probe during the FSW process, and then grain

refinement occurs as a consequence of dynamic recrystallization. The grain size, however, increases with the tool rotation speed. In general, the size of dynamically recrystallized grains decreases with the increase of strain and/or strain rate. Here we observe that the grain size increases in spite of the increase in the tool rotation speed, which is expected to lead to the increase in the strain and strain rate. We also observe that some additional static grain growth occurred in the SZ during cooling after severely plastically deformed by the rotating probe, because the maximum temperature of the SZ increased with the increase of tool rotation speed.

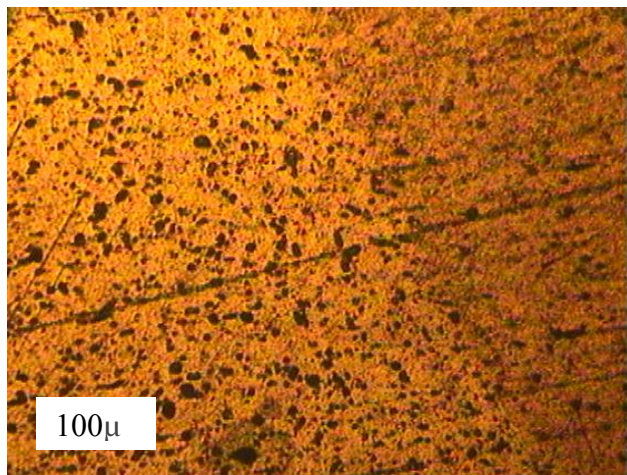


**Fig.9e** Optical microstructures of the stir zone (SZ) with rotating speed 1000 rpm (square profile).

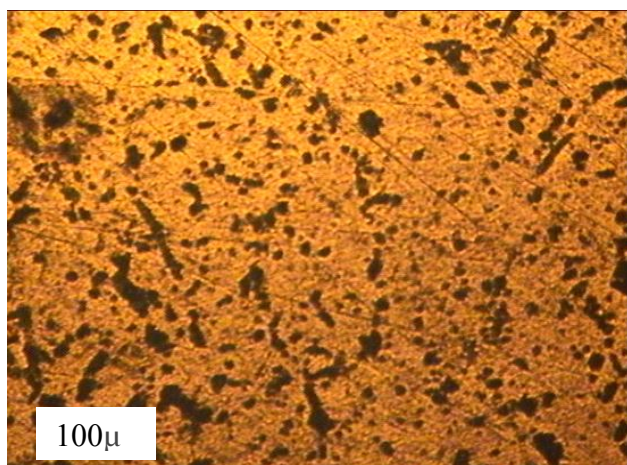


**Fig.9f** Optical microstructures of the stir zone (SZ) with rotating speed 1400 rpm (square profile).

The stir zone (SZ) appears as an ellipse type and onion rings pattern, which is observed in the SZ, was formed by the process of friction heat owing to the rotation of the tool and the forward movement extrudes the metal around to the retreating side of the tool. The welding flash is only released at the retreating side, where the direction of the tool rotation moves oppositely to the travel direction (anti-parallel). The transition regions are formed between the SZ and unaffected base metals (BM). It can be seen from all micrographs that the grains in the nuggets of all FSW welds are much finer than these in parent materials.

The central part of the weld zone (along the tool centerline) is observed to be dynamically recrystallized. This is typical of all friction stir welding processes examined in dissimilar metal systems.

Typical micrographs showing the dispersion of second-phase in both alloys are in Fig. 9(b). Particles of several intermetallic phases are present in the alloys. The majority of the particles are phases containing the usual impurities of Al, i.e., Fe and Si and the alloying elements Mg, Mn, Zn, Si. The phases  $\alpha$ -Al<sub>12</sub>(Fe,Mn)<sub>3</sub>Si, Al<sub>6</sub>(Fe,Mn) and Mg<sub>2</sub>Si are present in AA5083 sheets. The alloy AA6082 contains phases containing Fe, Si and Cu, i.e. Al<sub>7</sub>Cu<sub>2</sub>Fe, and also the phases Al<sub>2</sub>CuMg, Mg<sub>2</sub>Si and (Zn,Cu,Al)<sub>2</sub>Mg. The particles of intermetallic phases are coarse and this indicates that all used materials were prepared from direct-chill cast alloys. The coarse insoluble intermetallic particles present in Al alloys are usually harder than the matrix. As FSW induces considerable heating, the aluminium matrix becomes even more plastic and easily flows around the particles. As a result, the process of FSW does not affect the shape and size of these particles. While FSW does not affect intermetallic particles, the stirring and heating of the material from both sides of joining line significantly changes the features of grain structure. In many cases, the macro-structure of weld cross-section presents a picture shown in the scheme in Fig. 9(c). Three zones with different microstructure and properties can be distinguished: a) nugget; b) thermo-mechanically affected zone (TMAZ); c) heat affected zone (HAZ).

Due to the intense plastic deformation and high temperature exposure within the stirred zone during FSW, recrystallization and texture development, as well as precipitate dissolution and coarsening, occur within and around the stirred zone. This feature has attracted extensive attention on the microstructural evolution of the weld joint. We focus on shape of nugget zone, nugget grain size, recrystallization mechanisms, dissolution and coarsening of the precipitates, weld texture. Generally, the weld joint can be divided into several zones, such as the nugget zone (NZ), the thermal-affected zone (TMAZ), and the heat-affected zone (HAZ). In the NZ, the metal around the FSW tool suffers greatly from the high temperature and strong stirring and forging, so the microstructures often have superfine equiaxial grain structures. The temperature in the NZ is also sufficiently high to lead to the dissolution of the precipitates. In the TMAZ adjacent to the NZ, dynamic recovery and recrystallization of some deformed and broken grains often occur due to the local heat cycle and non-homogenous strains. Grain size in the TMAZ is larger than that in the NZ. Similarly, the relatively high temperature causes the dissolution or growth of some precipitates and a decrease in the mechanical properties of the weld joints. In the HAZ, where only heat is applied, the precipitates and grains only coarsen if the temperature is high enough. Softening often occurs in the HAZ, because of the decrease in the volume fraction of the precipitates.

### 3.3 Micro Hardness

If the measured hardness indenter were located more near a primary phase than near eutectic Al/Si, the hardness is

about 75 HV, but in the opposite case, the hardness of the BM shows over 90 HV. The hardness of specimens depends on the measured point of the hardness indenter. However, the hardness of the SZ shows more uniform values than that of the BM due to finer and uniformly dispersed Si particles.

The improvement of the mechanical properties of the joint by FSW can be attributed to two reasons. The eutectic Si particles are more homogeneously distributed in the stir zone than in the base metals. Therefore, the hardness distribution of the stir zone is also uniform compared with that of the base metals, which has a scattered value due to the heterogeneous distribution of eutectic Si particles. The main reason for improvement of mechanical properties in the stir zone is strengthening by the fully dispersed fine Si particles.

The base material has a Vickers hardness of about 130 HV, very high for an alloy of this type. However, the welding process softens the material significantly with the hardness reducing by nearly 50% around the weld line to about 75 HV. The hardness does not seem to have been influenced by the change in pin geometry, probably due to the dominant influence of the tool shoulder on the thermal input during welding. The variations in hardness mentioned above can be readily correlated with the microstructure developed both during and after the welding process. It is most convenient to describe the microstructure in terms of the three main regions apparent in the hardness profiles; the softened region around the weld line, the unaffected parent material and a transition region between them. The 5xxx series alloys are predominantly work hardenable alloys and so it is this microstructure, typical of rolling/work hardening that is the main contributor to the high hardness of this region compared to the weld zone.

**Table 10:** Results of hardness tests of FSW joints for different cutting tools

Sample ID	Al-alloy	
	Square cutting tool profile	Cylindrical cutting tool profile
	(1000rpm)	(1000rpm)
1mm	75.3	85.4
2mm	75	85.4
3mm	74	84
4mm	67.4	72.5
5mm	64.7	78.4
6mm	62.4	77.6
7mm	57.9	76.8
8mm	56.5	80.3
9mm	54.6	80.7
10mm	53.4	81
11mm	53.2	81.8
12mm	53.6	82.2
13mm	55.2	81.4
14mm	70.6	79.4
15mm	80.8	59
16mm	85.1	52.1
17mm	87.9	48.6
18mm	88.1	50
19mm	87.7	51.5

20mm	87	56
21mm	86.5	48.7
22mm	79.6	57.1
23mm	79	60.2
24mm	80.6	52.1
25mm	80.9	60.8

These show that the welding process has dramatically altered the microstructure of the material in this region. The heavily worked microstructure of the base material has been completely replaced by equiaxed grains around 10–13 μm in diameter that have little sub-structure, typical of a recrystallized microstructure and similar to that found previously in 5xxx, 6xxx and 7xxx series aluminium stir welds.

The width of 6082 Al alloys layer is wider than that of 5083 Al alloy. The region which was dominant structure of the stir zone showed fine and equiaxed grain structure of 6082 Al alloy and no scars of 5083 Al alloy. The center region of the stir zone showed macroscopically swirl and vortex-like patterns of each material, microscopically recrystallized 6082 Al alloys and thinly distributed Si particles. Above table shows the cross-sectional hardness profile near the weld zone according to the fixed location of materials. Hardness of the stir zone was lower than that of 6082 Al alloy, but higher than that of 5083 Al alloy. The softening of the stir zone in case of precipitate hardened Al alloy like 6082 Al alloys mainly due to the precipitates behaviour during the welding thermal cycle. The improved hardness of the stir zone in case of 5083 Al alloys was caused by homogeneously distributed Si particles. The hardness of the stir zone showed higher value in case 6082 Al alloys were fixed at the retreating side. This result can be explained by the dominant microstructure of the stir zone.

A hardness decrease occurs when approaching the TMAZ. The average hardness of the nugget zone (NZ) was found to be significantly lower than the hardness of the base alloy. There is a zone outside the nugget (transition between TMAZ and HAZ) which has the lower hardness value. The variation of the micro hardness values in the welded area and parent material is due to the difference between the microstructures of the base alloy and weld zone. Hardness in the dissimilar joints presented the lower values of all parent metals. The hardness in the nugget area is similar for all joints and it is always higher than the values in the transition between the TMAZ and the HAZ. The hardness depends on the precipitate distribution such as Mg<sub>2</sub>Si. It is likely that the low hardness can be attributed to the re-solution of the precipitates during friction stir welding.

For the as weld specimen the profile indicates a higher hardness in the nugget region compared to the base material. This is because the as received parent material was in the homogenized condition wherein all the precipitates are dissolved, thus accounting to a lower hardness due to the absence of strengthening precipitates. In the nugget region, which experiences higher temperatures than the remaining regions, the dissolved precipitates do re-precipitate subsequently. Here the precipitates are finer and uniformly distributed in the

nugget region. Increase in speed rate results decrease in hardness. Also micro-hardness profile in the table indicate that hardness at SZ is more than other zones and far from centre joint line at TMAZ and its boundary with HAZ hardness decrease, in both RS and AS, and after that increase till parent metal hardness. TMAZ and its boundary with HAZ have minimum hardness, i.e. the zone where defect free joints fail in tensile test. The average hardness decrease with speed rate increasing; it is because of softening take place at SZ. It can be said that heat input increase during welding results hardness decreasing. Rotating speed is more effective than feed rate in this case. Friction stir welding is caused to decreasing of the displacement density and de-creasing in that cause to decreasing of the micro hardness. In this process tool rotation and feed rate cause to dynamic recrystallization and dynamic recrystallization cause to new grain giant.

### Conclusions

Aluminum alloys 5083 and 6082 were successfully joined by friction stir welding (FSW) and the most favorable welding conditions among those tested were identified. The joints properties of friction-stir-welded Al 5083 and Al 6082 alloys were studied with various tool rotating speeds and different tool pin profiles with constant traverse speed (20mm/min). The following conclusions have been derived.

- 1) Most favorable friction stir weld parameters over a tested range were established. The choice takes into consideration surface finish, minimum internal defect, and no crack formation and tensile strength, while maximizing tool rotation speed within FSW machine constraints.
- 2) The friction stir welding process results in significant grain refinement of the alloy in the weld.
- 3) The microstructures of dissimilar formed Al 5083 and Al 6082 alloys joint showed the mixed structures of two materials. The onion ring pattern, which appeared like lamellar structure, was observed in the stir zone. Superior tensile properties of FSW joints were observed, this is due to the formation of fine equiaxed grains and uniformly distributed very fine strengthening precipitates in the weld region.
- 4) Sound joints were acquired at 20 mm/min welding speed when the tool rotating speed was fixed at 1000 rpm for both circular and square tool pin profiles. The dendrite structures, which are characteristic in the base metal (BM), disappeared and showed the dispersed eutectic Si particles in the stir zone (SZ).

- 5) The rapid recrystallization is favored at the top of the weld, where contact with the tool shoulder occurred. This region experiences the highest deformation, highest temperature, and most wear debris.
- 6) Recrystallisation results in the weld zone having considerably lower hardness and yield stress than the parent base metals. During tensile testing, almost all the plastic flow occurs within the recrystallized weld zone.
- 7) The transverse ultimate and yield strength had similar values with the BM. All the specimens were fractured at the unaffected BM.

### References

- N.BhanodayaKiranBabu, A.Prabhu Kumar and M.Joseph Davidson(2011), A Review of Friction-stir Welding of AA6061 Aluminium Alloy,*Journal of Engineering and Applied Sciences*,vol 6,no.4, pp.61-64
- P.M.G.P.Moreira,T.Santos,S.M.O.Tavares,V.Richter-Trummer,P.Vilaça,P.M.S.T.deCastro(2009),Mechanical and metallurgical characterization of friction stir welding joints of AA6061-T6 with AA6082-T6,,*Materials & design*,vol 30,pp.180-187
- S. Sattari, H.Bisadi, M.Sajed(2012), Mechanical Properties and Temperature Distributions of Thin Friction Stir Welded Sheets of AA5083, *International Journal of Mechanicals and Applications*,vol 2,no.1,pp.1-6
- Won-BaeLee,Yun-Mo Yeon,Seung-Boo Jung(2003),The joint properties of dissimilar formed Al alloys by friction stir welding according to the fixed location of materials,*ActaMaterialia*,,vol 49,pp.423-428
- C.G.Rhodes, M.W.Mahoney, W.H.Bingel, M.Calabrese, Fine-grain evolution in friction-stir processed 7050 aluminum,*Scr. Mater.*48,1451
- Olga Valerio Flores,ChristineKennedy,L.E. Murr,David Brown,SridharPappu, Brook M. Nowak and J.C. McClure(1998), Micro Structural Issues in friction Stir Welded aluminum alloy, *ScriptaMaterialia*, Vol. 38, No. 5,pp.703-708
- Murr L.E., Brown D. and McClure J.C.,1999,Flow visualization and residual micro structures associated with the friction stir welding of 2024 aluminum to 6061 aluminum, *ScriptaMaterialia*, Vol. 271, pp. 213-223
- Hidetoshi Fujii,LingCui,MasakatsuMaeda,KiyoshiNogi,2006,Effect of tool shape on mechanical properties and microstructure of friction stir welded aluminum alloys.*Material Science Engineering Applications*, 419: pp.25-31